Signature of special behaviours of $1/r^2$ interaction in the quantum entanglement entropy

2012 J. Phys. A: Math. Theor. 45 425302

(http://iopscience.iop.org/1751-8121/45/42/425302)

IOP Publishing Journal of Physics A: Mathematical and Theoretical

J. Phys. A: Math. Theor. **45** (2012) 425302 (13pp) doi:10.1088/1751-8113/45/42/425302

Signature of special behaviours of $1/r^2$ interaction in the quantum entanglement entropy

Poulomi Sadhukhan and Somendra M Bhattacharjee

Institute of Physics, Bhubaneswar, 751 005, India

E-mail: poulomi@iopb.res.in and somen@iopb.res.in

Received 22 July 2012, in final form 10 September 2012
Published 8 October 2012
Online at stacks.iop.org/JPhysA/45/425302

Abstract

We study the bipartite von Neumann entropy of two particles interacting via a long-range scale-free potential $V(r) \sim -g/r^2$ in three dimensions, close to the unbinding transition. The nature of the quantum phase transition changes from critical ($-3/4 < g < 1/4$) to first order ($g < -3/4$) with $g = -3/4$ as a multicritical point. Here, we show that the entanglement entropy has different behaviours for the critical and the first-order regimes. But there still exists an interesting multicritical scaling behaviour for all $g \in (-2 < g < 1/4)$ controlled by the $g = -3/4$ case.

PACS numbers: 03.65.Ud, 05.30, Rt, 64.70.Tg, 87.14.gk

(Some figures may appear in colour only in the online journal)

1. Introduction

Quantum entanglement [1–4] is an important aspect of quantum mechanics that tells us about the quantum correlation of two particles or subsystems spatially apart. When a composite quantum system is in a pure non-product state, even if the subsystems are spatially far apart and non-interacting, the measurement of one subsystem affects that of the other instantaneously. This 'spooky action at a distance' later gave birth to the term 'entanglement'. This phenomenon was first marked by Einstein, Podolsky and Rosen in a gedanken experiment [5], known as the EPR paradox. In their paper, they considered two particles which interacted for some time and showed that it is possible to measure the conjugate non-commutating quantities, such as position and momentum, simultaneously, in violation of quantum mechanics. Later, it was resolved and resulted in the idea of quantum entanglement which indicates the presence of inherent quantum effects, not just correlations, between the two particles In fact, quantum entanglement is a resource for quantum computation with no classical counter-part. Here, in this paper, we consider two interacting particles in a pure state, like an EPR pair, or more specifically in the two-particle ground state, in which case we can expect to observe the entanglement.

A quantum phase transition (QPT) occurs at zero temperature, and at the QPT, the ground-state energy is non-analytic with respect to some parameter in the Hamiltonian. A QPT is fully governed by quantum fluctuations, and hence, one would expect that the quantum entanglement would show special signatures at the QPT, even it is found that the entanglement entropy behaves in different ways for a first-order and a continuous transition. The critical behaviour of the entanglement entropy draws much attention nowadays [6] and has been investigated for different spin models [1, 2, 7] as well as in continuum systems [8].

To quantify the entanglement, various definitions of entanglement entropy are used, among which the von Neumann entropy [1, 2, 6, 7] is the most common. Recently, it was shown that the von Neumann entropy of two particles has a $d \ln \kappa$ behaviour at the quantum critical point (QCP) of unbinding in dimensions $1 < d < 4$. This has been established analytically for a 3D potential well [9]. Here, the QCP is attained when the inverse length scale κ, the inverse of the width of the wavefunction, approaches zero. This is achieved by tuning the potential or the mass. Also, it is shown that this divergence is essential for the criticality and linked to the reunion behaviour of two polymers in the equivalent classical statistical mechanical problem of polymers. In this paper, we study how the von Neumann entropy for a long-range potential, like $1/r^2$, changes as one varies its strength and sign. The equivalent classical statistical mechanical problem involves two directed polymers interacting at the same contour length like a DNA with native base pairing but with an additional $1/r^2$ interaction. The polymer model has been studied using a renormalization group in [10, 11].

This paper considers two particles interacting through a three-dimensional inverse square law potential and finds the quantum entanglement between the particles. Here, we use particle partitioning [6]. The Hamiltonian for the two particles we shall be using is

$$H = \frac{\mathbf{p}_1^2}{2m_1} + \frac{\mathbf{p}_2^2}{2m_2} + V(\mathbf{r}_1 - \mathbf{r}_2), \tag{1}$$

where m_i, $\mathbf{r}_i$ and $\mathbf{p}_i$ are the mass, the position and the momentum of the ith particle;

$$V(r) = \begin{cases} -V_0, & \text{for} \quad r < a, \quad (V_0 > 0), \\ -\dfrac{2\mu}{\hbar^2}\dfrac{g}{r^2}, & \text{for} \quad r > a, \end{cases} \tag{2}$$

is a central potential; and $\mu = m_1 m_2/(m_1 + m_2)$ is the reduced mass of the two particles. We take $2\mu/\hbar^2 = 1$.

The inverse square potential is of immense importance in quantum mechanics [12]. It is at the boundary of the short-range and the long-range potentials. For potentials decaying like r^{-p} in three dimensions, there is no finite bound state if $p > 2$, while for a slower divergence, i.e. $p < 2$, there is a finite negative lower bound in energy. For an attractive potential $-g/r^2$ ($g > 0$), the kinetic and the potential energies are of the same order near small r and so the bound-state spectrum depends on the value of g. A manifestation of the borderline case is in the scale-free nature, $H(\lambda r) = \lambda^{-2} H(r)$. This makes g the dimensionless strength of the potential, i.e. a 'marginal' parameter in the RG sense in all dimensions. The singularity of g/r^2 at the origin prevents discrete bound states. A suitable modification of the potential at small r, e.g., by putting a cutoff and replacing the potential by a short-range finite attraction near origin, gives discrete bound states. This is given in equation (2).

It is established in quantum mechanics that there is no finite-energy ground state for $g > 1/4$. For $g < 1/4$, the wavefunction is normalizable and the bound-state energy can be obtained by the standard procedure. In this regime of g, the unbinding transition is induced by tuning the strength of the short-range potential near $r = 0$, depicting the QPT. The unbinding transition in this long-range interaction is a unique example of a QPT whose type can be of first order ($g < -3/4$), critical but non-universal ($g > -3/4$), and even of the Kosterlitz–Thouless

Table 1. Conversion table for g–λ. Real values of λ occur for $g <\leqslant 1/4$.

g	-2	$-3/4$	0	$1/4$	$> 1/4$
λ	1.5	1	1/2	0	Imaginary

type ($g = 1/4$) [11]. The solvability and the wide repertoire of QPT behaviour make this model an ideal terrain for exploration of the nature of entanglement entropy around a QPT.[1] This is what we set to do in this paper.

A phase transition is defined as a singularity in the energy, associated with diverging length scales. In this sense, the quantum unbinding transition is a genuine phase transition. This QPT exists because the time of infinite extent plays a role in quantum mechanics. It becomes clear in the path integral formulation. The quantum problem can be mapped onto an equivalent classical statistical mechanical problem of polymers under the imaginary time transformation ($it \to N$). The time in the quantum problem then becomes the length of the polymer N, Green's function maps on to the partition function and the ground-state energy corresponds to the free energy per unit length. The interaction between the polymers means the interaction of a pair of monomers at the same index along the length of the polymers as in DNA base pairing. This is equivalent to the same time interaction of two quantum particles. The equivalent classical problem in the context of melting transition of two polymers interacting via a potential like equation (2) has been discussed in [10] which reveals that the results of the quantum problems can be recovered from such studies. Like the quantum particle making excursion inside and outside of the well, the polymers also come closer, reunite and move further, forming swollen bubbles. The entropy of a bubble of length N is

$$\ln \Omega(N) = N\sigma_0 - \Psi \ln N, \tag{3}$$

where $\Omega(N)$ is the reunion partition function of two polymers starting together, reuniting anywhere in space again at length N, σ_0 is the bubble entropy per unit length and Ψ is the reunion exponent. The details can be found in [9, 10, 13].

The binding–unbinding transition of polymers, for DNA melting, has been studied in the context of the necklace model of polymers and it is found that the reunion exponent Ψ determines the order of transition [13]. The phase transition occurs if $\Psi \geqslant 1$. The transition is continuous if $1 < \Psi < 2$, while it is of first order for $\Psi > 2$. In three dimensions, the reunion exponent is given by [10]

$$\Psi = 1 + \lambda, \quad \text{with} \quad \lambda = \sqrt{\frac{1}{4} - g}, \tag{4}$$

where the dependence on g, a bit counter-intuitive, is a consequence of its marginality. Here also we use the parameter $\lambda(> 0)$ because of its occurrence in what follows. Table 1 gives the correspondence between g and λ for easy reference.

The phase diagram and the lines of RG fixed points are shown in figure 1. This plot shows the phases in the g–u plane, where

$$u = -V_0\, a^2, \tag{5}$$

in the unit of $2\mu/\hbar^2 = 1$, is the dimensionless short-range potential, in which the two-particle state is in. The fixed points shown here are obtained from the renormalization group analysis

[1] What makes the unbinding transition special is the change in the topology of the underlying space. Note that the wavefunction $|\psi\rangle$ belongs to a space $H_B \to H_c \otimes H_2$, where H_c is the Hilbert space for a free particle and H_2 is the separable space of square integrable functions. This space for the bound state goes over to the space $H_U = H_c \otimes H_c$ for two particles (scattering states). Another way of observing this is via currents. The space H_B allows only one current for the CM, while H_U allows two currents for the two unbound particles. In this paper, we stay in the H_B space on the bound side.

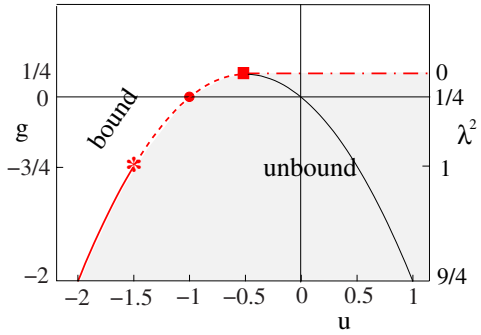

Figure 1. g versus u phase diagram. The plot shows the phases and the RG fixed points in the g–u plane ($u = -V_0\, a^2$). The red curve below $g = 1/4$ and $u = -0.5$ shows the binding–unbinding transitions governed by a line of unstable real fixed points. The transition is of first order for $g < -3/4$ and of second order for $-3/4 < g < 1/4$. This line is the transition line in the limit of zero range potential ($a \to 0$, $V_0 \to \infty$, with u =constant). The black continuous curve for $u > -0.5$ shows the locus of stable fixed points representing the unbound phase. The dash–dotted line at $g = 1/4$ is the boundary beyond which the fixed points are complex.

performed in [10]. The red line for $u < -0.5$ shows the unstable fixed points across which the unbinding transition takes place, and the black continuous line for $u > -0.5$ shows the phases by stable fixed points. For $g < -3/4$, the bound–unbound transition is of first order for $\Psi > 2$, which is indicated by the red continuous line ending at the symbol * at $g = -3/4$, or, $\lambda = 1$, a multicritical point. After that the transition is continuous up to $g = 1/4$ with $\Psi < 2$. Beyond that, where λ is imaginary, there is no real fixed point, and the system is in a bound state. Across the $g = 1/4$ line, with $u \geqslant -0.5$, a Kosterlitz–Thouless-type phase transition from the bound state to the unbound state can be induced by tuning g. The two regimes, $\Psi < 2$ and $\Psi > 2$, are governed by different behaviours, with additional log-corrections at $\Psi = 2$.

We find that the entanglement entropy also carries this signature of the speciality of $g = -3/4$ or $\lambda = 1$. The entropy in the three different regimes, $\lambda < 1$, $\lambda = 1$ and $\lambda > 1$, scale in different manners. We establish that $\lambda = 1$ behaves like a multicritical point for the entanglement entropy too, controlling both the first-order and the critical behaviour in the whole range $-2 \leqslant g \leqslant 1/4$.

The outline of the rest of the paper is as follows. In section 2, we describe our model and the method by which we calculate the von Neumann entropy. The analytical results are presented in section 3 and the von Neumann entropy is calculated for $\lambda < 1$. Next, we present the exact numerical results obtained using MATHEMATICA and discuss the behaviour of the entropy and its scaling in section 4. Finally, we conclude the paper in section 5.

2. Model and method

Equation (2) is used for our study. The detailed nature of the short-range potential is not important and we take it as a simple square-well potential. We concentrate in the range $0 < \lambda < 3/2$.

The von Neumann entropy (S) is defined as

$$S = -\mathrm{Tr}\,(\rho \ln \rho), \tag{6}$$

where ρ is the reduced density matrix for the ground state $|\psi\rangle$ of a two-particle system,

$$\rho(\mathbf{r}_1, \mathbf{r}_1') = \mathrm{Tr}_2\, \varrho(1,2) = \int \mathrm{d}^3\mathbf{r}_2\, \langle \mathbf{r}_1, \mathbf{r}_2|\psi\rangle\langle\psi|\mathbf{r}_1', \mathbf{r}_2\rangle, \tag{7}$$

obtained from the two-particle density matrix $\varrho(1,2) = |\psi\rangle\langle\psi|$ by integrating out particle 2. The density matrix in $\ln\rho$ is to be made dimensionless by appropriate powers of cut-off a.

As the interaction is translationally invariant, the reduced density matrix $\rho(\mathbf{r},\mathbf{r}') \equiv \rho(\mathbf{r}-\mathbf{r}')$ satisfies the eigenvalue equation [9]

$$\int \mathrm{d}^3\mathbf{r}'\ \rho(\mathbf{r}-\mathbf{r}')\exp(-\mathrm{i}\mathbf{q}\cdot\mathbf{r}') = \hat{\rho}(\mathbf{q})\exp(-\mathrm{i}\mathbf{q}\cdot\mathbf{r}). \tag{8}$$

The eigenfunction is $\exp(-\mathrm{i}\mathbf{q}\cdot\mathbf{r})$ with the eigenvalue

$$\hat{\rho}(\mathbf{q}) = |\phi(\mathbf{q})|^2, \tag{9}$$

where we have put the centre of mass (CM) wave vector to be zero without loss of generality. Here, $\phi(\mathbf{q})$ is the normalized momentum-space wavefunction of the relative co-ordinate. Therefore, the von Neumann entropy reads

$$S = -\int \mathrm{d}^3\mathbf{q}\ |\phi(\mathbf{q})|^2\ \ln|\phi(\mathbf{q})|^2. \tag{10}$$

The reduced density matrix in the basis of momentum states $|\mathbf{k}\rangle$ has the form

$$\rho = \int \mathrm{d}^3\mathbf{k}\ |\phi(\mathbf{k})|^2\ |\mathbf{k}\rangle\langle\mathbf{k}| \stackrel{\text{def}}{=} \int \mathrm{d}^3\mathbf{k}\ \frac{\mathrm{e}^{-\beta H_{\text{ent}}}}{Z}\ |\mathbf{k}\rangle\langle\mathbf{k}|, \tag{11}$$

which makes the mixed-state characteristic explicit. Equation (11) allows us to define ρ as a thermal density matrix with an entanglement Hamiltonian H_{ent} at a fictitious inverse temperature β with Z being the partition function. This thermal correspondence makes the von Neumann entropy equivalent to the Gibbs entropy of H_{ent}.

In equation (11), H_{ent} is a c-number. Consider the canonical partition function of a free particle at temperature T: $Z \sim \int \mathrm{d}^d q \exp(-\beta H) \sim T^{d/2}$, where $H = \hbar^2 q^2/2m$. Then, the entropy becomes $S = \ln Z \sim \ln T$, which for very low temperature, $T \to 0$, becomes negative. In another way, one obtains a constant specific heat C from the equipartition theorem, which then gives a logarithmic dependence on temperature of the entropy: $S = \int^T (C/T)\mathrm{d}T \sim \ln T$. The Sackur–Tetrode constant, the dimensionless entropy of one mole of an ideal gas at temperature $T = 1$ K and one atmospheric pressure, is a fundamental constant [15]. Its value is $-1.164\,8708$. Note that this fundamental entropy is negative. A classical harmonic oscillator is no exception. It is well known that the condition $S \geqslant 0$ does not hold for the classical continuous statistical mechanics [16].

3. Analytical results

In this section, we derive the asymptotic behaviour of $\phi(q)$. In particular, we find that the entropy is dominated by the outer part, i.e. the excursion in the classically forbidden region, if the unbinding transition is critical. This happens for $0 < \lambda \leqslant 1$. For first-order transition, the inner part also contributes significantly.

To find out the von Neumann entropy of two interacting particles in the ground state, we first write the wavefunction as a product of that for the CM and for the relative coordinate

$$\psi(\mathbf{r}_1,\mathbf{r}_2) = \Phi(\mathbf{R})\,\varphi(\mathbf{r}), \tag{12}$$

where Φ and φ are the wavefunction in the CM and relative coordinates, respectively, defined by

$$\mathbf{R} = \frac{m_1\mathbf{r}_1 + m_2\mathbf{r}_2}{m_1+m_2} \quad \text{and} \quad \mathbf{r} = \mathbf{r}_1 - \mathbf{r}_2. \tag{13}$$

We proceed with the radial part putting the CM momentum as zero. The CM is completely delocalized in space.

The ground state has zero angular momentum, and therefore, only the radial part of $\varphi(\mathbf{r})$, i.e. $R(r)$, in the spherical polar coordinate is needed. For this s-state, the radial part of the Schrödinger equation then reads [14]

$$\frac{\partial^2 R}{\partial r^2} + \frac{2}{r}\frac{\partial R}{\partial r} + (V_0 + E)R = 0, \quad \text{for } r < a, \tag{14}$$

and

$$\frac{\partial^2 R}{\partial r^2} + \frac{2}{r}\frac{\partial R}{\partial r} + \left(\frac{g}{r^2} + E\right)R = 0, \quad \text{for } r > a, \tag{15}$$

where E is the ground-state energy of the particle describing the behaviour of the two particles in a relative coordinate.The radial part of the wavefunctions in the relative coordinate is then obtained by solving equations (14) and (15):

$$R(r) = \begin{cases} \dfrac{A}{r}\sin kr, & \text{for } r \leqslant a, \qquad (16a) \\ \dfrac{B}{\sqrt{r}}H_\lambda^{(1)}(\mathrm{i}\kappa r), & \text{for } r \geqslant a, \qquad (16b) \end{cases}$$

where A and B are the normalization constants, $H_\lambda^{(1)}$ is the Hankel function of first kind and

$$k^2 = V_0 - |E|, \quad \kappa^2 = |E|. \tag{17}$$

We choose λ to be positive and it is given by equation (4). In the limit of $\kappa \to 0$, the unbinding transition takes place. This makes our interest in studying the von Neumann entropy in this limit.

At $r = a$, the continuity of the wavefunctions gives

$$\frac{A}{a}\sin ka = \frac{B}{\sqrt{a}}H_\lambda^{(1)}(\mathrm{i}\kappa a), \tag{18}$$

and the matching condition of the derivative of the wavefunction gives

$$ak\cot ak = \mathrm{i}\kappa a\frac{H_{\lambda-1}^{(1)}(\mathrm{i}\kappa a)}{H_\lambda^{(1)}(\mathrm{i}\kappa a)} - \lambda + \frac{1}{2}, \tag{19}$$

which determines the value of k for a given κ. Given the values of λ and a, one can obtain the threshold or the minimum value of k, i.e. k_m, for just one bound state. For $\kappa = 0$,

$$ak_c\cot ak_c = \tfrac{1}{2} - \lambda \tag{20}$$

is the condition for the transition point when the ground-state energy $E \to 0$. Equation (20) has always a solution for $\lambda \geqslant 0$.

Now consider a small deviation from the critical value of k, $k = k_c - \delta$, where $\delta \sim V_0 - V_c$. Then, from equation (19),

$$(ak_c - a\delta)\cot(ak_c - a\delta) \sim \begin{cases} (\kappa a)^{2\lambda}, & \text{for} \quad \lambda < 1, \\ (\kappa a)^2, & \text{for} \quad \lambda > 1, \end{cases} \tag{21}$$

or

$$|E| = \kappa^2 \sim \begin{cases} \delta^{1/\lambda}, & \text{for} \quad 0 < \lambda < 1, \\ \delta + O(\delta^{1/(\lambda-1)}), & \text{for} \quad \lambda > 1. \end{cases} \tag{22}$$

These show that as $V_0 \to V_c \equiv k_c^2$, E remains continuous, as it should. For $\lambda < 1$, E approaches zero tangentially, while for $\lambda > 1$, there is a nonzero slope at $\kappa = 0$. This discontinuity of slope classifies the $\lambda > 1$ transition as first order. Despite that, the higher derivatives on the bound side $\partial^n E/\partial\delta^n$ would show divergences like a critical point.

The normalization constants A and B are obtained by using the continuity condition and taking the limit $\kappa \to 0$ (see the appendix for details):

$$|A|^2 \sim \begin{cases} (a\kappa)^{2-2\lambda}/a, & \text{for } \lambda < 1, \\ 1/a, & \text{for } \lambda > 1, \end{cases} \tag{23}$$

and

$$|B|^2 \sim \begin{cases} \kappa^2, & \text{for } \lambda < 1, \\ \kappa^2 (a\kappa)^{2\lambda-2}, & \text{for } \lambda > 1. \end{cases} \tag{24}$$

At $\lambda = 1$, there are log corrections which we do not get into here. The log correction appears in the necklace model for polymers whenever the reunion exponent Ψ (equation (4)) is an integer. The log appears in equation (19) via $H_0^{(1)}$ for $\lambda = 1$. Now, one knows the full wavefunction and its limiting κ behaviour.

The reduced density matrix has the eigenvalues $|\phi(\mathbf{q})|^2$, where $\mathbf{q}$ is the momentum space variable. To obtain these eigenvalues, the Fourier transformation of the wavefunction needs to be performed:

$$\phi(q) = \frac{1}{(2\pi)^{3/2}} \int \mathrm{d}^3 r \, \mathrm{e}^{\mathrm{i}\mathbf{q}\cdot\mathbf{r}} R(r) = \phi_{\mathrm{i}}(q) + \phi_{\mathrm{o}}(q), \tag{25}$$

where the subscripts 'i' and 'o' refer to the inner ($r < a$) and the outer ($r > a$) parts. The Fourier transform of the inner part (equation (16*a*)) is

$$\phi_{\mathrm{i}}(q) = \frac{A}{q} \frac{1}{\sqrt{2\pi}} \left[\frac{\sin(k-q)a}{k-q} - \frac{\sin(q+k)a}{q+k} \right] \tag{26}$$

and of the outer part (equation (16*b*)) is

$$\begin{aligned} \phi_{\mathrm{o}}(q) = |B| \, \kappa^{-5/2} \, \frac{\sqrt{2}}{\pi} \, \Gamma\left(\frac{5}{4} + \frac{\lambda}{2}\right) \Gamma\left(\frac{5}{4} - \frac{\lambda}{2}\right) {}_2F_1\left(\frac{5}{4} + \frac{\lambda}{2}, \frac{5}{4} - \frac{\lambda}{2}; \frac{3}{2}; -\frac{q^2}{\kappa^2}\right) \\ - |B| \int_0^a \mathrm{d}r \sqrt{r} \frac{\sin qr}{q} K_\lambda(\kappa r), \end{aligned} \tag{27}$$

where ${}_2F_1$ is the hypergeometric function and K_λ is the modified Bessel function. The last integral in equation (27) is convergent for all $\lambda < 1$ and therefore can be ignored in the $\kappa \to 0$ limit.

The limiting small κ dependence of the inner and the outer parts of the wavefunction from equations (26) and (27), respectively, is of the form

$$\phi_{\mathrm{i}}(q) = \begin{cases} (a\kappa)^{1-\lambda} a^{3/2} f_{\mathrm{i}}(aq), & \text{if } \lambda < 1, \\ a^{3/2} f_{\mathrm{i}}(aq), & \text{if } \lambda > 1, \end{cases} \tag{28}$$

and

$$\phi_{\mathrm{o}}(q) = \begin{cases} \kappa^{-\frac{3}{2}} f_\lambda(q/\kappa), & \text{if } \lambda < 1, \\ \kappa^{-\frac{3}{2}} (a\kappa)^{\lambda-1} f_\lambda(q/\kappa), & \text{if } \lambda > 1, \end{cases} \tag{29}$$

where f_{i} and f_λ are the well-behaved functions. Equation (28) is for large q.

From equations (28) and (29), we see that the double limit $\kappa \to 0$, $\lambda \to 1$ is singular because of the term $(a\kappa)^{1-\lambda}$. The dependence of entropy on the order of the limits is discussed later on. This identifies $(\kappa = 0, \lambda = 1)$ as a special point. From this, we also identify $(1-\lambda)\ln(a\kappa)$ as an appropriate scaling variable. This scaling variable will occur below in the analysis of the numerical results.

For $\lambda < 1$, i.e. $1 - \lambda > 0$, $(a\kappa)^{1-\lambda} \to 0$ as $\kappa \to 0$, and therefore, the contribution of outer part dominates over the inner part in the von Neumann entropy. Without much loss, one can then write the entropy with the outer part only (equation (29)):

$$\begin{aligned} S &\approx -\int \mathrm{d}^3 q \, |\phi|^2 \ln |\phi_{\mathrm{o}}|^2 \\ &= 3 \ln a\kappa + c_\lambda, \quad (\text{for} \quad \lambda < 1) \end{aligned} \tag{30}$$

with

$$c_\lambda = \int \mathrm{d}x\, x^2 f_\lambda(x) \ln f_\lambda(x). \tag{31}$$

We introduced a in equation (30) to make the argument of ln dimensionless, mentioned earlier. As per our interest, we extract the κ-dependent term and call the rest c_λ, which is a function of other parameters. The main result is that there is a log divergence of S as $\kappa \to 0$.

4. Exact numerical results

To study the nature of the entanglement entropy, over the whole range of λ we take recourse to exact numerical calculation using MATHEMATICA for the three-dimensional potential well. We cross-check our prediction of equation (30) and then show a multicritical scaling that covers the range $0 < \lambda < 3/2$.

4.1. Protocol

Although V_0 is the tuning parameter, it is more convenient to use the length scale as the independent parameter. With this treading of κ for V_0, our protocol is as follows: given the values of κ and λ, the value of k_m was determined from equation (19), with $k_m < \pi$ that assures us the ground state. As $\kappa \to 0$, $k_m \to k_c$. Then, the corresponding normalization coefficients A and B were found by using the normalization condition and the continuity equation, i.e. by performing the r-integrations of the inner and the outer parts of the wavefunction in equation (A.2). These constants are used in the Fourier transformed inner and outer parts of the wavefunction, equations (26) and (27), to calculate the von Neumann entropy. In the final integration for $S = -\mathrm{Tr}\,\rho \ln \rho$, we put an upper cut-off making sure that the final numbers are independent of this choice of cut-off. Also the intervals of the integration range have carefully been chosen especially for $q \sim \kappa$. This gives numerically exact numbers for the entropy for the given κ and λ. This procedure is repeated for various λ and κ. We set $a = 1$.

4.2. Behaviour of the von Neumann entropy S

4.2.1. λ dependence. The plots of the numerical values of the von Neumann entropy S against $\ln \kappa$ and λ show different behaviours of entropy in different ranges of λ, namely $\lambda < 1$, $\lambda > 1$ and $\lambda = 1$.

Let us first look at the plot of S versus λ in figure 2, where different lines represent different values of κ. For $\lambda < 1$, the von Neumann entropy for small κ saturates to a negative value as λ is varied and that the saturation value depends on the value of κ. The smaller the value of κ, the more negative the entropy, and $\kappa \to 0$ takes the saturation value to negative infinity. The long-range part of the potential is attractive for $\lambda > 0.5$ and repulsive otherwise. But the entropy shows no signature as it crosses $\lambda = 0.5$. On the other hand, for $\lambda > 1$, where the transition becomes of first order, the entropy does not decrease much with κ, rather becomes independent of κ. It remains finite for $\lambda > 1$ and diverges at $\lambda = 1$ like the black dashed curve in figure 2. S becomes positive at $\lambda \sim 1.3$. It seems that this point has no significance otherwise.

4.2.2. κ dependence. The behaviour of the von Neumann entropy with λ and κ becomes more clear when one looks at the plot of S versus κ (figure 3). This plot shows the different characteristic behaviours of S in the three distinct ranges of λ: $\lambda < 1$, $\lambda = 1$ and $\lambda > 1$. For small κ, all $\lambda < 1$ curves have slope 3 when plotted against $\ln \kappa$, i.e. for $\lambda < 1$, the entropy is

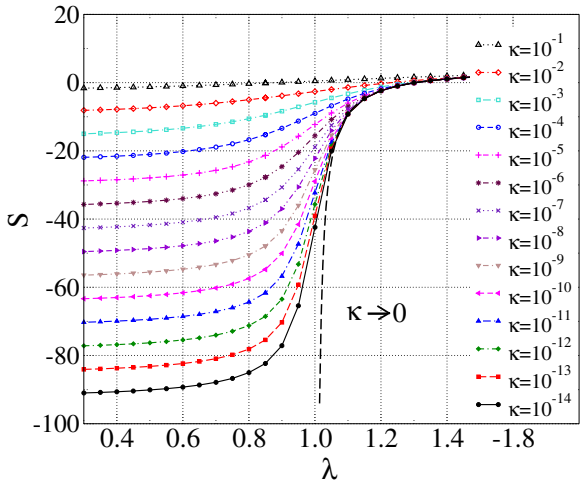

Figure 2. S versus λ for various κ. The plot shows that the entropy diverges for $\lambda \leqslant 0$ as $\kappa \to 0$. The dashed line marked as $\kappa \to 0$ is the expected behaviour of the entropy for $\lambda > 1$.

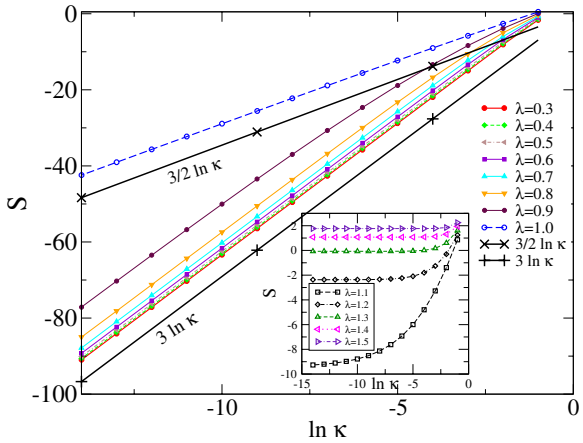

Figure 3. S versus $\ln \kappa$ for various λ. For comparison, $3 \ln \kappa$ and $\frac{3}{2} \ln \kappa$ are shown by black lines with the symbols $+$ and $\times$. The inset shows that the entropy is κ-independent for $\lambda > 1$.

of the expected form $3 \ln \kappa + c_\lambda$ which is shown from analytical calculations. To obtain $3 \ln \kappa$, one has to see below some value of κ, and as λ approaches one, even smaller κ needs to be considered. But no matter how close to 1 the value of λ is, one obtains $3 \ln \kappa$ until $\lambda < 1$. Exactly at $\lambda = 1$, the slope changes suddenly to $3/2$, and hence,

$$S = \tfrac{3}{2} \ln \kappa + c_1, \quad \text{for} \quad \lambda = 1. \tag{32}$$

A somewhat different behaviour is observed for the rest with $\lambda > 1$ (the inset of figure 3). For small κ, the curves reach a λ-dependent constant value and do not change with κ. Clearly, the entropy has no κ dependence for $\lambda > 1$ and it is finite. By definition, these constant values are c_λ and $S(\lambda > 1) = c_\lambda$. So, we see that there are three classes:

$$S = \begin{cases} 3 \ln \kappa + c_\lambda, & \text{for } \lambda < 1, \\ \frac{3}{2} \ln \kappa + c_1, & \text{for } \lambda = 1, \\ c_\lambda, & \text{for } \lambda > 1. \end{cases} \tag{33}$$

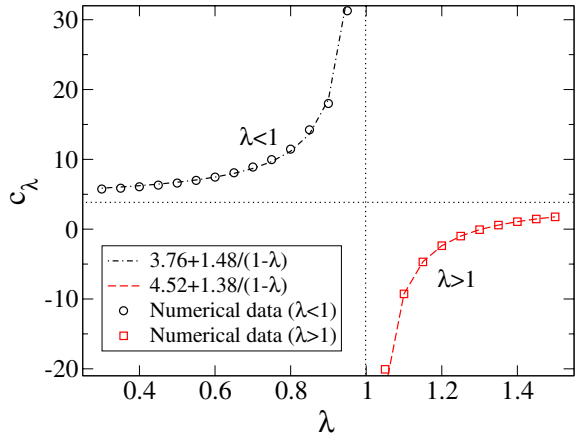

Figure 4. The plot of c_λ versus λ, showing a divergence at $\lambda = 1$.

4.2.3. On c_λ. Now we have knowledge of the κ-dependent part in the von Neumann entropy for different λ. The next question is how c_λ behaves with λ, and if they have a different nature in different regimes of λ. So, we collect the c_λ according to equation (33), except for $\lambda = 1$, and plot against λ. This plot (figure 4) shows a divergence at $\lambda = 1$ indicating that $(1 - \lambda)$ is an important quantity. The data points are fit into the function

$$c_\lambda = m + n/(1 - \lambda), \tag{34}$$

via m and n, and the fitted set of parameters are (4.52, 1.38) and (3.76, 1.48) for λ greater and less than 1, respectively. The divergence of c_λ at $\lambda = 1$ leads to the possibility of a reduction of the slope of S from 3 to 3/2 when plotted against $\ln \kappa$.

4.2.4. Data collapse. We noted that for $\lambda > 1$, c_λ, and hence the entropy itself, has a $(1 - \lambda)$ dependence, and for $\lambda < 1$, the entropy has a $\ln \kappa$ term with $c_\lambda = f(1 - \lambda)$. It was pointed out in section 3, below equation (29), that $(1 - \lambda) \ln \kappa$ seems to be a scaling variable. We therefore look at the plot of the entropy versus $(1 - \lambda) \ln \kappa$. The entropy has different behaviours on the two sides of the $\lambda = 1$ making it a special point. Also, it has a separate scaling behaviour. This drives us to plot $(S_\lambda - S_1)/(\frac{3}{2} \ln \kappa)$ against $(1 - \lambda) \ln \kappa$. We see a good data collapse (see figure 5) for various sets of data of figure 2. Hence, one can write the scaling form of von Neumann entropy:

$$(S_\lambda - S_1)/\tfrac{3}{2} \ln \kappa = \mathcal{F}((1 - \lambda) \ln \kappa). \tag{35}$$

Figure 5 shows that $(S_\lambda - S_1)/\frac{3}{2} \ln \kappa$ reaches $+1$ for small enough κ for $\lambda < 1$ and -1 for $\lambda > 1$. Once we obtain the scaling behaviour of the entropy at $\lambda = 1$, the same away from this special point can also be obtained.

5. Discussion and conclusion

In this paper, we studied the von Neumann entropy S, the most common measure of the entanglement entropy, for an inverse square potential in three dimensions. The entropy behaves in different ways for three different ranges of modified interaction strength λ and given by equation (33). For $\lambda < 1$ and $\lambda = 1$, the entropy has a diverging nature as one approaches QCP by tuning κ. The behaviour of entropy is completely different for $\lambda > 1$, where the κ

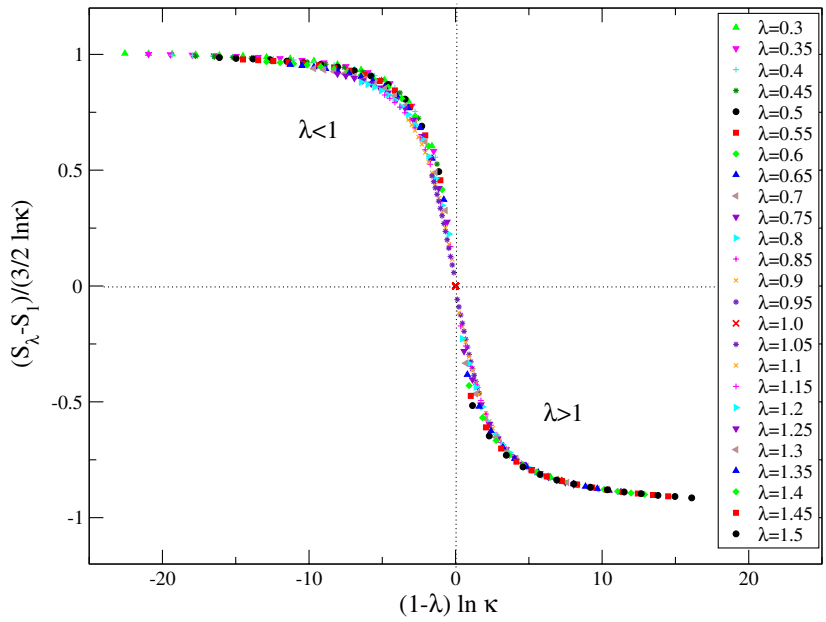

Figure 5. Data collapse: $(S_\lambda - S_1)/\frac{3}{2}\ln\kappa$ versus $(1-\lambda)\ln\kappa$.

dependence of the entropy vanishes. There is a $\frac{1}{1-\lambda}$ divergence in the entropy. These three distinct classes collapse onto a single curve when $(S_\lambda - S_1)/\frac{3}{2}\ln\kappa$ is plotted against $(1-\lambda)\ln\kappa$. This data collapse indicates that there is a common scaling behaviour of the entropy for any λ and that $\lambda = 1$ is special. Because of the diverging factor dependence on $(1-\lambda)$, one has to be careful in taking a required limit of $\kappa \to 0$ as the one that would give a log correction in entropy for $\lambda = 1$. For $g > 1/4$, λ is imaginary which we do not consider here. In this paper, we focused on the multicritical point at $\lambda = 1$. There is one more multicritical point at $\lambda = 0$ with the KT transition. This case will be discussed elsewhere. It would be interesting to study the entanglement behaviour for a discretized version of the model.

The nature of the divergence of the entanglement entropy at $\lambda = 1$ depends on the path of approaching $\lambda = 1$ in a λ–κ plane. Diagrammatically, it has been shown in figure 6. If we take the limit $\kappa \to 0$ first and then $\lambda = 1$, the entropy diverges like $1/(1-\lambda)$ (shown by the red line in figure 6(*a*)), and like $\ln\kappa$ for the other way around (see the blue line in figure 6(*b*)). For $\lambda < 1$, the $\kappa \to 0$ line corresponds to $S = -\infty$, but for $\lambda > 1$ the same line gives a finite value for entropy. The path dependence of figure 6 summarizes the features of the entanglement entropy, with $\lambda = 1, \kappa = 0$ as a special point controlling the behaviour in its neighbourhood. The data collapse of figure 5, then, suggests that the paths should be classified by the constant value of $X = (1-\lambda)\ln\kappa$.

For $\lambda < 1$, restricting to the critical case, we see $\rho(q) \sim |\phi(q)|^2$. These are the eigenvalues of the density matrix. Now the reduced density matrix ρ describes a mixed state, though the full ground state is pure. Being a mixed state, we may represent ρ as a 'thermal' density matrix, $\rho \sim \exp(-\beta H_{\rm ent})$, as given in equation (11). Since the entanglement spectrum is known, we have

$$\beta H_{\rm ent} \approx \ln|{}_2F_1|^2 \approx \frac{1}{2}\frac{q^2}{\kappa^2}, \quad \text{for } q \to 0, \tag{36}$$

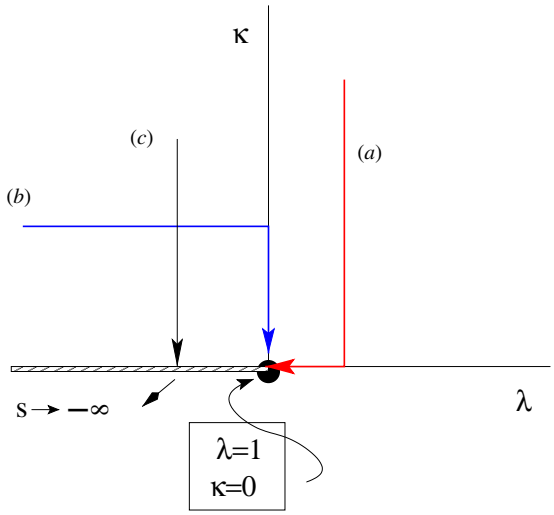

Figure 6. The path dependence of entropy. Two different limits of approaching $\{\lambda = 1, \kappa \to 0\}$. (*a*) First $\kappa \to 0$ and then $\lambda = 1$ (red line). The entropy diverges like $1/(1-\lambda)$. (*b*) First $\lambda \to 1$ and then $\kappa \to 0$ (blue line). The entropy diverges like $\ln \kappa$. Thick line along *x*-axis for $\lambda \leqslant 1$ denotes divergent entropy. (*c*) For $\lambda < 1$, taking the limit $\kappa \to 0$ (black vertical line with arrow) leads to divergent entropy and *S* remains so along the horizontal stretch.

identifying $\beta = 1/\kappa^2$ and $H_{\rm ent} = q^2/2$. As mentioned before, for this $H_{\rm ent}$, the Gibbs entropy is $\sim \frac{\rm d}{2} \ln T$. Since in this case $T \simeq \kappa^2$, we find the von Neumann entropy $S \sim d \ln \kappa$.

Appendix. Calculation of the normalization constants *A* and *B*

The normalization constants A and B are found by using the continuity condition and taking limit $\kappa \to 0$ in the normalization condition,

$$4\pi \left[\int_0^a |A|^2 \sin^2 kr \, {\rm d}r + \int_a^\infty r |B H_\lambda^{(1)}({\rm i}\kappa r)|^2 \, {\rm d}r \right] = 1. \tag{A.1}$$

Replacing A by B, by using the continuity equation, i.e. equation (19), we obtain

$$\left[\left(2\pi a - \frac{\pi}{k} \sin 2ak \right) \frac{a \left| H_\lambda^{(1)}({\rm i}\kappa a) \right|^2}{\sin^2 ka} + 4\pi \int_a^\infty r \left| H_\lambda^{(1)}({\rm i}\kappa r) \right|^2 {\rm d}r \right] |B|^2 = 1. \tag{A.2}$$

Now we use the form of the Hankel function in the limit $\kappa \to 0$,

$$\left| H_\lambda^{(1)}({\rm i}\kappa r) \right|^2 \sim \frac{2^\lambda \Gamma^2(\lambda)}{\pi^2} (\kappa r)^{-2\lambda}, \tag{A.3}$$

and rewrite the outer part integral in the normalization condition in a simpler form, namely

$$\begin{aligned} \int_{\kappa a}^\infty r \left| H_\lambda^{(1)}({\rm i}r) \right|^2 {\rm d}r &= \int_{\kappa a}^1 \left[|H_\lambda^{(1)}({\rm i}r)|^2 - \frac{2^\lambda \Gamma^2(\lambda)}{\pi^2} r^{-2\lambda} \right] {\rm d}r \\ &\quad + \int_{\kappa a}^1 \frac{2^\lambda \Gamma^2(\lambda)}{\pi^2} r^{-2\lambda} \, {\rm d}r + \int_1^\infty r \left| H_\lambda^{(1)}({\rm i}r) \right|^2 {\rm d}r \\ &= \frac{\Gamma^2(\lambda)}{\pi^2 2^{1-\lambda}} \frac{1 - (a\kappa)^{2(1-\lambda)}}{1-\lambda} + \cdots . \end{aligned} \tag{A.4}$$

Putting equations (A.4) and (A.3) in equation (A.2), one obtains

$$|B|^2 = \frac{\pi}{2^{\lambda+1}\Gamma^2(\lambda)}\left[\left(\frac{\lambda^2 + a^2k^2 - 1/4}{k^2}\right)(a\kappa)^{-2\lambda} + \frac{1}{\kappa^2}\frac{1-(a\kappa)^{2(1-\lambda)}}{(1-\lambda)}\right]^{-1}, \tag{A.5}$$

which in the extreme limit of $\kappa \to 0$ gives the κ dependence of B:

$$|B|^2 \sim \begin{cases} \kappa^2, & \text{for } \lambda < 1, \\ \kappa^2(a\kappa)^{2\lambda-2}, & \text{for } \lambda > 1. \end{cases} \tag{A.6}$$

Once B is obtained, the κ dependence of the other constant A can be found by using equation (18) as

$$|A|^2 \sim \begin{cases} (a\kappa)^{2-2\lambda}/a, & \text{for } \lambda < 1, \\ 1/a, & \text{for } \lambda > 1. \end{cases} \tag{A.7}$$

References

[1] Bose I and Chattopadhyay E 2002 *Phys. Rev.* A **66** 062320
[2] Vidal G *et al* 2003 *Phys. Rev. Lett.* **90** 227902
[3] Horodecki R *et al* 2009 *Rev. Mod. Phys.* **81** 865
[4] Amico L *et al* 2008 *Rev. Mod. Phys.* **80** 517
[5] Einstein A, Podolsky B and Rosen N 1935 *Phys. Rev.* **47** 777
[6] Calabrese P, Cardy J and Doyon B 2009 *J. Phys A: Math. Theor.* **42** 500301 and see, e.g., the articles in the special issue
[7] Osterloh A 2002 *Nature* **416** 608
[8] Dehesa J S 2012 *J. Phys. B: At. Mol. Opt. Phys.* **45** 015504
[9] Sadhukhan P and Bhattacharjee S M 2012 *Europhys. Lett.* **98** 10008
[10] Mukherji S and Bhattacharjee S M 2001 *Phys. Rev.* E **63** 051103
[11] Kolomeisky E B and Straley J P 1992 *Phys. Rev.* B **46** 12664
[12] Landau L D and Lifshitz L M 2004 *Quantum Mechanics Non-Relativistic Theory* 3rd edn (Amsterdam: Butterworth-Heinemann)
[13] Fisher M E 1984 *J. Stat. Phys.* **34** 667
[14] van Haeringen H 1978 *J. Math. Phys.* **19** 2171
[15] Mohr P J, Taylor B N and Newell D B 2008 *Rev. Mod. Phys.* **80** 633
[16] Lieb E H and Ruskai M B 1973 *Phys. Rev. Lett.* **30** 434